Authors' Camera Ready Manuscript. To appear in the
Proceedings of the 23rd IEEE International Conference on Industrial Technology, Shanghai, China, Aug 2022.
Please cite using bibliographic data of the associated published version.

Modelling and controller design for a five-link inverted pendulum

Yarong Zhou
School of Naval Architecture, Ocean & Civil Engineering
Shanghai Jiao Tong University
Shanghai, China
yarong.zhou@sjtu.edu.cn

Parijat Bhowmick
Department of Electronics and Electrical Engineering
Indian Institute of Technology Guwahati
Guwahati, India
parijat.bhowmick@iitg.ac.in

Ying Fu
Department of Electrical and Electronic Engineering
University of Manchester
Manchester, UK.
Ying.Fu2@boschhuayu-steering.com

Ye Li
School of Naval Architecture, Ocean & Civil Engineering
Shanghai Jiao Tong University
Shanghai, China
ye.li@sjtu.edu.cn

Alexander Lanzon
Department of Electrical and Electronic Engineering
University of Manchester
Manchester, UK.
Alexander.Lanzon@manchester.ac.uk

***Abstract*—The inverted pendulum is a fast-moving, highly nonlinear and unstable system with multiple variables and non-minimum phase that requires effective stabilization controllers. Therefore, studies into inverted pendulum systems theoretically and practically have great significance. The Euler-Lagrange Equation is used to calculate the mathematical model for a five-link inverted pendulum system. Linear Quadratic Gaussian (LQG) and $\mathcal{H}_\infty$ are implemented using the developed model, with the Kalman Filter serving as the observer. The closed-loop system are simulated by the Matlab-Simscape platform and the controller are evaluated in relation to the system performance.**

***Index Terms*—Five-link inverted pendulum, Euler-Lagrange modelling, $\mathcal{H}_\infty$ control, LQG, observer-based controller, Kalman filter.**

I. Introduction

Inverted pendulums are ideal experimental tools in the control theory research due to their typical factors such as higher-order, higher-sensitivity, multiple variables and strong coupling. It is used to reflect representative problems and determine whether the controller or control theory is capable of dealing with the corresponding problems. The inverted pendulum system was first studied in the 1950s. The cybernetics experts at Massachusetts Institute of Technology (MIT) designed a single inverted pendulum experiment based on rocket launch principles [1]. Subsequently, researches on the double link inverted pendulum for humanoid robots were conducted [2]. As the industrial equipment becomes more complicated and closes up to large-scale, the inverted pendulum with multi-link demonstrates its potential to represent a wide variety of industrial frontier problems. In the field of the wind turbine [3], it can act as preliminary fundamental research for problems such as control for the mooring system of floating wind turbine equipped in deep water over rated conditions [4].

The mathematical model of a single inverted pendulum is easy to access due to its low cost of calculation. For higher-order system, Jadlovska and Sarnovsky(2013) [5] deduced a inverted pendulum with three joints in detail and also introduced the mathematical modelling of generalized inverted pendulum systems. A variety of controllers have been tried to stabilize inverted pendulum systems with a single or double links. For instance, by linearizing the model at the equilibrium point, classic control methods such as Proportion-Integration-Differentiation (PID), pole placement, Linear Quadratic Regulator (LQR) and model predictive control (MPC) have been implemented with inverted pendulums [6]–[8]. Sliding mode variable structure control [9] and adaptive control combined with other control methods [10] have been adopted to stabilize this system. Intelligent control methods which are independent of the linear mathematical model like neural networks [11] and Bat optimization [12] also showed their ability for the control of single inverted pendulum. However, as the sensitivity grows with the number of links, different emphasis requirements for controller performance are put forward.

In this paper, the mathematical model of higher-order inverted pendulum system is deduced and explicitly, and two controller are made for this highly sensitive system which

This work was supported by the Ministry of Science and Technology of China [2017YFE0132000].

are validated by Matlab-Simscape platform. The essential requirement for inverted pendulum control is the stabilization of the plant. Other abilities of controllers (e.g., reference tracking, noise and model perturbation rejection) will also be validated. This work will also be a prior test for properties analysis of controllers which may be adopted to wind turbine system.

II. Mathematical modelling

The kinetic model of the five-link pendulum is deduced under an ideal condition based on the Euler-Lagrange Equation, and transformed to a standard state equation by linearizing at the equilibrium point.

A. Structure and parameter definitions

The inverted pendulum system is complex and has a high requirement for response speed and the ability to deal with strong nonlinearity. To simplify the calculation of analysis, in the process of establishing the actual mathematical model [13], assumed that:

- Air resistance is ignored.
- The system is abstracted into a system consisting of a cart and a uniform rigid rod.
- All kinds of minor frictions resistance between rod and joint are ignored.
- The friction between the wheels of the cart and the ground is ignored.
- The ground is horizontal.

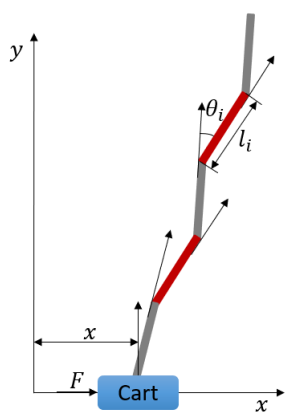

Fig. 1. The abstract physical model of five-link inverted pendulum.

The abstracted mechanical model of the system with a cart, uniform rigid rods and a mass block is shown as Fig. 1. From the bottom up, number rods by 1 to 5, and the relevant parameters are defined as the Table. I.

B. Mathematical models based on Euler-Lagrange Equation

Euler-Lagrange Equation [14] is used to describe the motion. In general, the Lagrange equation of motion is given by

$$\frac{\mathrm{d}}{\mathrm{d}t}\frac{\partial L}{\partial \dot{q}} - \frac{\partial L}{\partial q} = Q, \tag{1}$$

TABLE I
The parameter definitions of inverted pendulum

Parameter	Description	Value	Dimension
M	The mass of cart	1.3	kg
$m_i, i = 1,2,3,4$	The mass of each rod	0.2	kg
m_5	The mass of the top rod	0.16	kg
$L_i, i = 1,2,3,4,5$	The length of each rod	0.5	m
θ_1	The angle between the first rod and vertical direction	/	rad
$\theta_i, i = 2,3,4,5$	The angle between each rod and the former one	/	rad
x_c	The position of the cart	/	m
g	Gravity acceleration	9.8	$\mathrm{m/s^2}$

with q the vector of degrees of freedom, L the Lagrangian functional and Q the external forces applied to the system.

The energy of the inverted pendulum system is composed of two parts: kinetic energy and potential energy. The Lagrangian functional is defined as the difference between them. Assumed that the gravity centers are in the geometrical centers of the rods. The general form reads as

$$L = \sum T_i - \sum V_i, \tag{2}$$

$$V_i = m_i g h_i, \tag{3}$$

$$T_i = \frac{1}{2} m_i v_i^2 + \frac{1}{2} J_i \beta_i^2, \tag{4}$$

with T the kinetic energy for each link and the cart, V the potential energy of them, h is the height of the center of mass of link, v the linear velocity of the center of mass, J the moment of inertia, and β the angular velocity of links.

Define coordinates of the mass points of the cart ($i = 0$) and rods ($i \in \{1, 2, \ldots, 5\}$) as (x_i, y_i):

$$x_i = \begin{cases} x_{i-1} + a_{i-1} + a_i & i = 2,3,4,5 \\ x_c + a_1 & i = 1 \\ x_c & i = 0 \end{cases}, \tag{5}$$

$$y_i = \begin{cases} y_{i-1} + b_{i-1} + b_i & i = 2,3,4,5 \\ b_1 & i = 1 \\ 0 & i = 0 \end{cases}, \tag{6}$$

where

$$a_i = \frac{1}{2} L_i \sin \sum_{n=1}^{i} \theta_n, \;\; b_i = \frac{1}{2} L_i \cos \sum_{n=1}^{i} \theta_n.$$

The kinetic energy (T_i) and potential energy (V_i) of the links can be defined as:

$$T_i = \begin{cases} \frac{1}{2} m_i (\dot{x_i}^2 + \dot{y_i}^2) + \frac{1}{2} J_i (\dot{\sum_{n=1}^{i} \theta_n})^2 & i = 1,2,3,4,5 \\ \frac{1}{2} M \dot{x_i}^2 & i = 0 \end{cases}, \tag{7}$$

$$V_i = \begin{cases} m_i g y_i & i = 1,2,3,4,5 \\ 0 & i = 0 \end{cases}, \tag{8}$$

where

$$J_i = \frac{1}{3} m_i l_i^2.$$

Define q in Euler-Lagrange equation (1) as

$$\begin{aligned} q &= \begin{bmatrix} x_c & \sum_{i=1}^{1} \theta_i & \sum_{i=1}^{2} \theta_i & \sum_{i=1}^{3} \theta_i & \sum_{i=1}^{4} \theta_i & \sum_{i=1}^{5} \theta_i \end{bmatrix}^\top \\ &= \begin{bmatrix} x_c & \theta_a & \theta_b & \theta_c & \theta_d & \theta_e \end{bmatrix}^\top \end{aligned} \tag{9}$$

and the Lagrange equation for the system can be written in a more compact form as:

$$D(q)\ddot{q} + C(q)\dot{q} + G(q) = Hu, \tag{10}$$

where

$$D(q) = \begin{bmatrix} d_1 & d_2 \cos\theta_a & d_3 \cos\theta_b & d_4 \cos\theta_c & d_5 \cos\theta_d & d_6 \cos\theta_e \\ d_2 \cos\theta_a & d_7 & d_8 \cos(\theta_b - \theta_a) & d_9 \cos(\theta_c - \theta_a) & d_{10} \cos(\theta_e - \theta_a) & d_{11} \cos(\theta_e - \theta_a) \\ d_3 \cos\theta_b & d_8 \cos(\theta_b - \theta_a) & d_{12} & d_{13} \cos(\theta_c - \theta_b) & d_{14} \cos(\theta_d - \theta_b) & d_{15} \cos(\theta_e - \theta_b) \\ d_4 \cos\theta_c & d_9 \cos(\theta_c - \theta_a) & d_{13} \cos(\theta_c - \theta_b) & d_{16} & d_{17} \cos(\theta_d - \theta_c) & d_{18} \cos(\theta_e - \theta_c) \\ d_5 \cos\theta_d & d_{10} \cos(\theta_d - \theta_a) & d_{14} \cos(\theta_d - \theta_b) & d_{17} \cos(\theta_d - \theta_c) & d_{19} & d_{20} \cos(\theta_e - \theta_d) \\ d_6 \cos\theta_e & d_{10} \cos(\theta_e - \theta_a) & d_{15} \cos(\theta_e - \theta_b) & d_{18} \cos(\theta_e - \theta_c) & d_{20} \cos(\theta_e - \theta_d) & d_{21} \end{bmatrix}, \tag{11}$$

$$C(q) = \begin{bmatrix} 0 & -d_2 \sin\theta_a \dot{\theta}_a & -d_3 \sin\theta_b \dot{\theta}_b & -d_4 \sin\theta_c \dot{\theta}_c & -d_5 \sin\theta_d \dot{\theta}_d & -d_6 \sin\theta_e \dot{\theta}_e \\ 0 & 0 & -d_8 \sin(\theta_b - \theta_a)\dot{\theta}_b & -d_9 \sin(\theta_c - \theta_a)\dot{\theta}_c & -d_{10} \sin(\theta_d - \theta_a)\dot{\theta}_d & -d_{11} \sin(\theta_e - \theta_a)\dot{\theta}_e \\ 0 & d_8 \sin(\theta_b - \theta_a)\dot{\theta}_a & 0 & -d_{13} \sin(\theta_c - \theta_b)\dot{\theta}_c & -d_{14} \sin(\theta_d - \theta_b)\dot{\theta}_d & -d_{15} \sin(\theta_e - \theta_b)\dot{\theta}_e \\ 0 & d_9 \sin(\theta_c - \theta_a)\dot{\theta}_a & d_{13} \sin(\theta_c - \theta_b)\dot{\theta}_b & 0 & -d_{17} \sin(\theta_d - \theta_c)\dot{\theta}_d & -d_{18} \sin(\theta_e - \theta_c)\dot{\theta}_e \\ 0 & d_{10} \sin(\theta_d - \theta_a)\dot{\theta}_a & d_{14} \sin(\theta_d - \theta_b)\dot{\theta}_b & d_{17} \sin(\theta_d - \theta_c)\dot{\theta}_c & 0 & -d_{20} \sin(\theta_e - \theta_d)\dot{\theta}_e \\ 0 & d_{11} \sin(\theta_e - \theta_a)\dot{\theta}_a & d_{15} \sin(\theta_e - \theta_b)\dot{\theta}_b & d_{18} \sin(\theta_e - \theta_c)\dot{\theta}_c & d_{20} \sin(\theta_e - \theta_d)\dot{\theta}_d & 0 \end{bmatrix}, \tag{12}$$

$$G(q) = \begin{bmatrix} 0 & -f_1 \sin\theta_a & -f_2 \sin\theta_b & -f_3 \sin\theta_c & -f_4 \sin\theta_d & -f_5 \sin\theta_e \end{bmatrix}^\top \tag{13}$$

and $H = \begin{bmatrix} 1 & 0 & 0 & 0 & 0 & 0 \end{bmatrix}^\top$. (14)

The corresponding parameters are defined in Table II.

TABLE II
THE PARAMETER DEFINITIONS OF d_i AND f_i

d_1	$M + \sum_{i=1}^{5} m_i$	d_2	$l_1 m_1 + L_1 \sum_{i=2}^{5} m_i$
d_3	$l_2 m_2 + L_2 \sum_{i=3}^{5} m_i$	d_4	$l_3 m_3 + L_3 \sum_{i=4}^{5} m_i$
d_5	$l_4 m_4 + L_4 m_5$	d_6	$l_5 m_5$
d_7	$J_1 + m_1 l_1^2 + L_1^2 \sum_{i=2}^{5} m_i$	d_8	$2 l_1 l_2 m_2 + 4 l_1 l_2 \sum_{i=3}^{5} m_i$
d_9	$2 l_1 l_3 m_2 + 4 l_1 l_3 \sum_{i=4}^{5} m_i$	d_{10}	$2 l_1 l_4 m_4 + 4 l_1 l_5 m_5$
d_{11}	$2 l_1 l_5 m_5$	d_{12}	$J_2 + m_2 l_2^2 + L_2^2 \sum_{i=3}^{5} m_i$
d_{13}	$2 l_2 l_3 m_3 + 4 l_2 l_3 \sum_{i=4}^{5} m_i$	d_{14}	$2 l_2 l_4 + 4 l_2 l_5 m_5$
d_{15}	$2 l_2 l_5 m_5$	d_{16}	$J_3 + m_3 l_3^2 + L_3^2 \sum_{i=4}^{5} m_i$
d_{17}	$2 l_3 l_4 m_4 + 4 l_3 l_4 m_5$	d_{18}	$2 l_3 l_5 m_5$
d_{19}	$J_4 + m_4 l_4^2 + L_4^2 m_5$	d_{20}	$2 l_4 l_5 m_5$
d_{21}	$J_5 + m_5 l_5^2$	f_1	$g d_2$
f_2	$g d_3$	f_3	$g d_4$
f_4	$g d_5$	f_5	$g d_6$

C. State-space modelling

To obtain a state-space model, define the state vector

$$x_q = \begin{bmatrix} q & \dot{q} \end{bmatrix}^\top. \tag{15}$$

The governing equation based on (10) then appears to be

$$\dot{x_q} = \begin{bmatrix} 0 & I \\ 0 & -D^{-1}C \end{bmatrix} x_q + \begin{bmatrix} 0 \\ -D^{-1}G \end{bmatrix} + \begin{bmatrix} 0 \\ D^{-1}H \end{bmatrix} u. \tag{16}$$

Since the primary objective of the controller is to stabilize the inverted pendulum at an upright position, the nonlinear model can be linearized around $x_q = \mathbf{0}$.

The linearized state equation of the inverted pendulum system reads as

$$\dot{x_q} = A x_q + B u, \tag{17}$$

with the state matrix $A = \begin{bmatrix} 0 & I \\ -D(0)^{-1} \frac{\partial G(0)}{\partial q} & 0 \end{bmatrix}_{12 \times 12}$ and the input matrix $B = \begin{bmatrix} 0 \\ D(0)^{-1} H \end{bmatrix}_{12 \times 1}$.

We can rearrange the state vector as

$$x = \begin{bmatrix} x_c & \dot{x_c} & \phi_1 & \phi_2 & \phi_3 & \phi_4 & \phi_5 \end{bmatrix}^\top \tag{18}$$

where $\phi_i = \begin{bmatrix} \theta_i & \dot{\theta}_i \end{bmatrix}^\top \ \forall i \in \{1, 2, \ldots, 5\}$. The corresponding output equation is

$$y = Cx \tag{19}$$

where the output matrix $C \in R^{6 \times 12}$ contains the cart position x_c and the link angles $\theta_i \ \forall i \in \{1, 2, \ldots, 5\}$. Besides, u is the external force applied to the system, which is the input to the system.

III. OBSERVER AND CONTROLLER DESIGN

The procedures of designing the Kalman Filter, LQG and $\mathcal{H}_\infty$ controller are provided. For better reference tracking performance, Type-1 servo control scheme is introduced to the system. According to separation principle [15], the controller and the observer can be designed independently.

A. Kalman Filter

It is impractical to get every state information of a system from sensors for the reasons of economy and necessity. Observable systems usually equip with observers. Kalman Filter [16] is able to estimate the states in the presence of stochastic disturbance (i.e., process noise and measurement noise).

The linear time invariant (LTI) systems with white noise can be represented as

$$\begin{cases} \dot{x} = Ax + Bu + \nu_1 \\ y = Cx + \nu_2 \end{cases} \tag{20}$$

where the pair of (A, C) is detectable. ν_1 and ν_2 are the white noise process satisfying the following properties

$$\begin{aligned} E\left[\nu_1 \nu_1{}^\top\right] &= WW^\top = \bar{Q}, \\ E\left[\nu_2 \nu_2{}^\top\right] &= \bar{R}, \\ E\left[\nu_1 \nu_2{}^\top\right] &= 0, \end{aligned}$$

with $\bar{Q} \geq 0$ and $\bar{R} \geq 0$ and the pair (A, W) being controllable. Let $\bar{P} \geq 0$ satisfy the following algebraic Riccati equation

$$A\bar{P} + \bar{P}A^\top - \bar{P}C^\top \bar{R}^{-1} C\bar{P} + \bar{Q} = 0. \tag{21}$$

The optimal state observer is constructed as

$$\dot{\hat{x}} = A\hat{x} + Bu + L\left(y - C\hat{x}\right), \tag{22}$$

where $L = \bar{P}C^\top \bar{R}^{-1}$.

The Loop-transfer Recovery (LTR) [17] technique has been utilised to preserve some of the robustness properties that we cannot afford to lose while implementing the Kalman filter.

Assume that the feedback gain is K. The overall closed-loop system can be approximated as

$$K\left(sI - A + BK + LC\right)^{-1} LC\left(sI - A\right)^{-1} B \approx K\left(sI - A\right)^{-1} B, \tag{23}$$

as it is easy to show that if $L = \rho B$, then

$$\lim_{\rho \to \infty} K\left(sI - A + BK + \rho BC\right)^{-1} \rho BC\left(sI - A\right)^{-1} B = K\left(sI - A\right)^{-1} B. \tag{24}$$

Here, $K\left(sI - A + BK + LC\right)^{-1} L$ is the transfer function matrix of controller and $C\left(sI - A\right)^{-1} B$ is that of the plant.

Furthermore, if L is selected as the Kalman filter gain with the weighting matrices

$$\bar{Q} = BB^\top \text{ and } \bar{R} = \frac{1}{\rho} I, \tag{25}$$

then $L \approx \sqrt{\rho} B$ for large values of ρ.

B. LQG controller

Although linearized system is open-loop unstable, it is controllable at the equilibrium point. LQG controllers are implemented in many practical applications consisting of the LQR controller and Kalman filter. The state-space representation of the plant is given by

$$\begin{cases} \dot{x} = Ax + Bu, \\ y = Cx. \end{cases} \tag{26}$$

For LQR design, we need to minimize the cost function

$$J = \int_0^\infty \left(x^\top Qx + u^\top Ru\right) \mathrm{d}t. \tag{27}$$

The optimal state feedback control law is given by

$$u = -Kx \tag{28}$$

where $K = R^{-1}B^\top P$ is the optimal state feedback gain with $P = P^\top > 0$ being the unique solution to the following ARE

$$PA + A^\top P - PBR^{-1}B^\top P + Q = 0. \tag{29}$$

We have selected $R = 1$ as the inverted pendulum is a single input system, and the elements of the weight matrix

$$Q = \mathrm{diag}\{600, 0, 1950, 0, 300, 0, 200, 0, 100, 0, 100, 0\}$$

have been tuned to achieve the desired performance.

C. $\mathcal{H}_\infty$ controller based on LMI

Consider the generalized plant model in 4-block structure as

$$\begin{cases} \dot{x} = Ax + B_1 w + B_2 u \\ z = C_1 x + D_{11} w + D_{12} u \\ y = C_2 x + D_{21} w + D_{22} u \end{cases} \tag{30}$$

where w denotes the external disturbance, z represents the error (output) vector which we are interested in and y is the measurement vector. A, B_1, B_2, C_2 are dependent on the system, and D_{11}, D_{21}, D_{22} are zero matrices.

The corresponding closed-loop transfer function $T_{wz}(s)$ must satisfy $||T_{wz}(s)||_\infty < \gamma$ to achieve asymptotically stable, that is,

$$||(C_1 + D_{12}K)(sI - A - B_2K)^{-1}B_1 + D_{11}||_\infty < \gamma, \tag{31}$$

with γ a constant. The resultant static $\mathcal{H}_\infty$ control law is

$$u = -Kx, \tag{32}$$

where $K = WX^{-1}$ with W and X being the feasible solutions to the following minimization problem

$$\min_{\rho} \begin{bmatrix} (AX + B_2W)^\top + AX + B_2W & B_1 & (C_1X + D_{12}W)^\top \\ B_1^\top & -I & D_{11}^\top \\ C_1X + D_{12}W & D_{11} & -\rho I \end{bmatrix} < 0. \tag{33}$$

In the above, the corresponding minimum disturbance inhibition degree is $\sqrt{\rho}$.

D. Type-1 servo control scheme

When the tracking performance of a particular state is emphasized, it is necessary to introduce an integral action. Define $C_r \in R^{1\times 12}$ for the emphasized state. Then, the error of position can be represented by

$$e = r - C_r x, \tag{34}$$

where r is the reference position of the state.

The augmented system can be expressed as

$$\dot{z} = \begin{bmatrix} \ddot{x} \\ \dot{e} \end{bmatrix} = \begin{bmatrix} A & 0 \\ -C_r & 0 \end{bmatrix} \begin{bmatrix} \dot{x} \\ e \end{bmatrix} + \begin{bmatrix} B \\ 0 \end{bmatrix} \dot{u}. \tag{35}$$

The system and control law read as

$$\begin{cases} \dot{z} = \bar{A}z + \bar{B}\dot{u} \\ \dot{u} = -\bar{K}z. \end{cases} \tag{36}$$

Define

$$K = \begin{bmatrix} K_x & k_e \end{bmatrix}_{1\times 13} \tag{37}$$

thereby the input can be obtained as

$$u = -K_x x - k_e \int e \, \mathrm{d}t. \tag{38}$$

IV. Matlab Simulation

The Matlab-Simscape [18] platform is adopted for the simulation of the closed-loop system. The performances of controllers are validated under different initial conditions, model perturbations, position reference and the amplitudes of noise. Different from state-space modelling, the internal mechanics in each joint are involved in the plant, which will further validated the robustness of controllers.

A. Simscape modelling

The structures of this closed-loop system with controllers follow the same routine as Fig. 2.

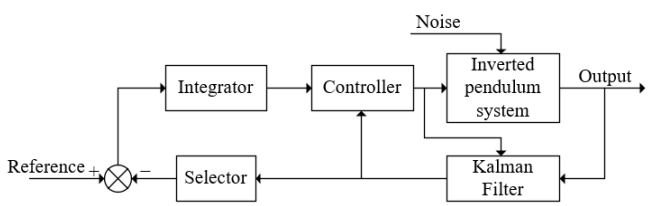

Fig. 2. The structure of closed-loop system.

The simulated link and plant are shown in Fig. 3(a) and Fig. 3(b). In the horizontal direction, the force is given to the cart as system input, and the white noise is given to the top of the upper rod as disturbance signal. The system output is the position of the cart and the angles of each rod with the front one.

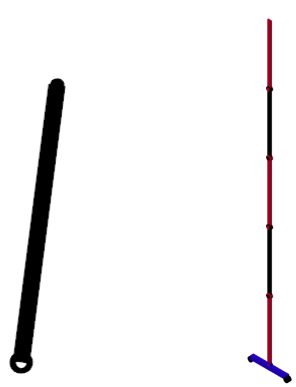

(a) (b)

Fig. 3. (a) Simulated link in Matlab-Simscape; and (b) Simulated 5-link inverted pendulum.

B. Simulation results

As is shown in Fig. 2, stabilization performances can be compared by changing the amplitude of white noise when the reference position is at the original point. P_n is used to represent noise power and the simulation duration is 60 seconds.

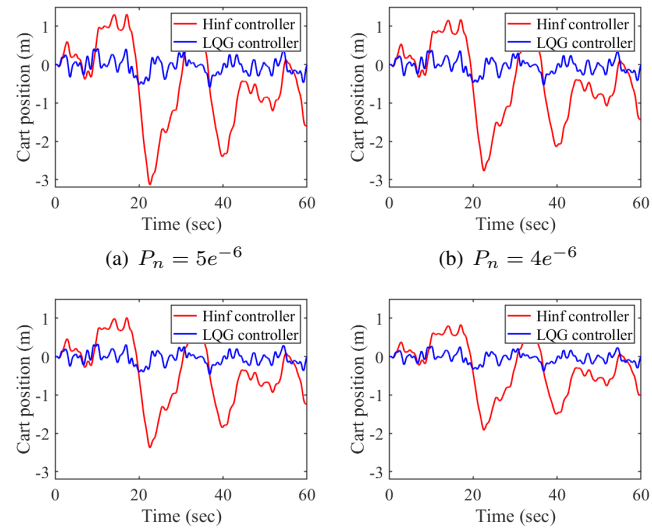

(a) $P_n = 5e^{-6}$ (b) $P_n = 4e^{-6}$

(c) $P_n = 3e^{-6}$ (d) $P_n = 2e^{-6}$

Fig. 4. Cart positions subject to different amplitudes of the noise signal.

Root mean square (RMS) is adopted to evaluate stabilization performances, and the results are shown in Fig. 5.

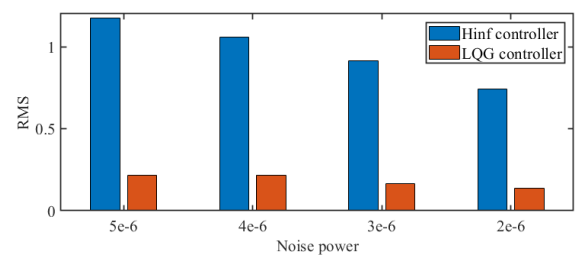

Fig. 5. RMS of several performances indices with $\mathcal{H}_\infty$(blue) and LQG (red).

It can be seen that the LQG controller stabilizes the inverted pendulum within a smaller displacement. From this point of view, the LQG controller is more applicable for stabilization under the circumstances that both of them can deal with noise rejection problems. Nevertheless, when the amplitude of white noise continues to increase, the inverted pendulum implemented with the LQG controller collapses, and that is to say, $\mathcal{H}_\infty$ controller can handle more extensive disturbances.

If there is no disturbance to the system, things are the same when the initial condition changes. Define θ_1 as the angle between the lowest link and the vertical position while other links are in the same line as their former. It is shown in Fig. 6 that, LQG controller spends a shorter time to stabilize the system with minor displacement. However, it can not work

as effectively as $\mathcal{H}_\infty$ controller when the operating point is further from the equilibrium point relatively.

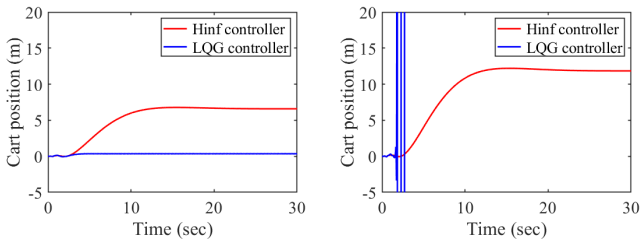

(a) $\theta_1 = 0.5°$ (b) $\theta_1 = 1°$

Fig. 6. Cart positions with different initial conditions.

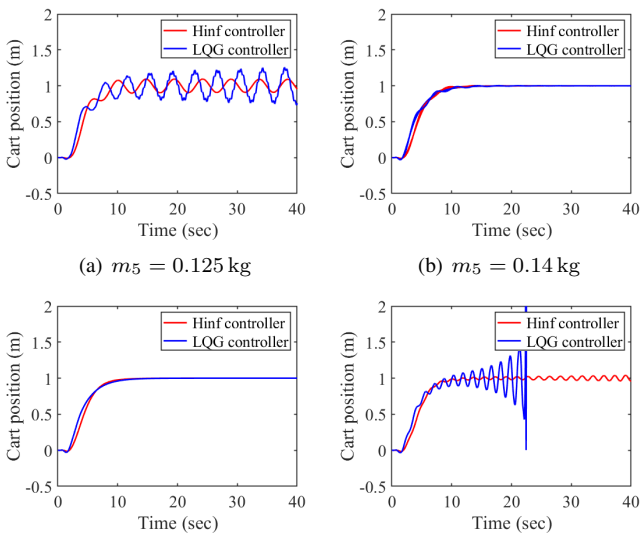

(a) $m_5 = 0.125\,\mathrm{kg}$ (b) $m_5 = 0.14\,\mathrm{kg}$

(c) $m_5 = 0.16\,\mathrm{kg}$ (d) $m_5 = 0.178\,\mathrm{kg}$

Fig. 7. Cart positions during reference tracking with different values of m_5.

Similarly, change the mass of the upper link m_5, and set the reference cart position to $1\,\mathrm{m}$. Integral actions are introduced to the two controllers following the routine of Type-1 servo control scheme. The matrix C_r is used to select position state. It is obvious that when $m_5 = 0.16\,\mathrm{kg}$, which is precisely the value in the modelling part, the LQG controller leads to shorter settling time. The changes of m_5 cause worse LQG controller performances in stabilization. When the change reaches a certain extent, the controller tends to fail. LQG controller exhibits satisfactory performance within a small range around the equilibrium point as the linearized model is close enough to the actual plant while $\mathcal{H}_\infty$ controller shows better robustness.

V. Conclusion

This work deduces the mathematical model of a five-link inverted pendulum with higher-sensitivity in detail based on the Euler-Lagrange equation. The proposed controllers equipped with a Kalman Filter are validated under the circumstances with different disturbances, model perturbations and uncertainties. LQG controller dependent on precise model exhibits satisfactory performance in stabilizing, while $\mathcal{H}_\infty$ controller meets the requirements of both disturbance rejection and model perturbation tolerance due to its good robustness. The visibility and reliability of simulation is improved by employing the Matlab-Simcape plant instead of the mathematical model as the experimental object.

In the future, we will implement these controllers in floating offshore wind turbine control for different purposes (e.g., load reduction and stabilization for platform and tower) according to their particular characteristics.

References

[1] K. H. Lundberg and T. W. Barton, "History of inverted-pendulum systems," *IFAC Proceedings Volumes*, vol. 42, no. 24, pp. 131–135, 2010.

[2] T. Sugihara, Y. Nakamura, and H. Inoue, "Real-time humanoid motion generation through ZMP manipulation based on inverted pendulum control," in *Proceedings 2002 IEEE International Conference on Robotics and Automation (Cat. No.02CH37292)*, 2002.

[3] K. A. Shah, F. Meng, Y. Li, R. Nagamune, and Z. Jiang, "A synthesis of feasible control methods for floating offshore wind turbine system dynamics," *Renewable and Sustainable Energy Reviews*, vol. 151, no. 1, p. 111525, 2021.

[4] P. A. Berthelsen, I. Fylling, L. Vita, and U. S. Paulsen, "Conceptual design of a floating support structure and mooring system for a vertical axis wind turbine," in *ASME 2012 31st International Conference on Ocean, Offshore and Arctic Engineering*, 2012.

[5] S. Jadlovska and J. Sarnovsky, "Modelling of classical and rotary inverted pendulum systems - a generalized approach," *Journal of Electrical Engineering*, vol. 64, no. 1, pp. 12–19, 2013.

[6] S. Cong, D. Zhang, and H. Wei, "Comparative study on three control methods of the single inverted-pendulum system," *Systems Engineering and Electronics*, 2001.

[7] L. B. Prasad, B. Tyagi, and H. O. Gupta, "Optimal control of nonlinear inverted pendulum system using PID controller and LQR: Performance analysis without and with disturbance input," *International Journal of Automation & Computing*, vol. 11, no. 006, pp. 661–670, 2014.

[8] T. Holzhüter, "Optimal regulator for the inverted pendulum via Euler–Lagrange backward integration," *Automatica*, vol. 40, no. 9, pp. 1613–1620, 2004.

[9] J. Hauser, A. Saccon, and R. Frezza, "On the driven inverted pendulum," in *European Control Conference and Conference on Decision & Control*, 2005.

[10] Y. Zhang, W. T. Ang, J. Jin, S. Zhang, and Z. Man, "Nonlinear adaptive sliding mode control for a rotary inverted pendulum," *advances in industrial engineering & operations research*, 2008.

[11] N. Metni, "Neuro-control of an inverted pendulum using genetic algorithm," in *International Conference on Advances in Computational Tools for Engineering Applications*, 2009.

[12] K. Srikanth and G. N. Kumar, "Stabilization at upright equilibrium position of a double inverted pendulum with unconstrained bat optimization," *International Journal of Computational Science*, vol. 5, no. 5, pp. 87–101, 2015.

[13] A. Gmiterko and M. Grossman, "An n-link inverted pendulum modeling," *Acta Mechanica Slovaca*, vol. 13, no. 3, pp. 22–29, 2009.

[14] O. P. Agrawal, "Formulation of Euler–Lagrange equations for fractional variational problems," *Journal of Mathematical Analysis & Applications*, vol. 272, no. 1, pp. 368–379, 2002.

[15] A. Loría and E. Panteley, *A separation principle for a class of Euler-Lagrange systems*. New Directions in nonlinear observer design, 1999.

[16] Q. I. Qian, L. I. Zu-Shu, Z. Tan, Y. H. Dan, and L. Xiao, "Noise suppression of inverted pendulum system based on Kalman filter," *Control and Decision*, 2010.

[17] A. Saberi and P. Sannuti, "Observer design for loop transfer recovery and for uncertain dynamical systems," *Automatic Control IEEE Transactions on*, vol. 35, no. 8, pp. 878–897, 1990.

[18] S. Yuan, Z. Liu, and X. Li, "Modeling and simulation of robot based on Matlab/SimMechanics," in *Control Conference*, 2008.